Published in final edited form as:

Nat Struct Biol. 2003 April ; 10(4): 250–255. doi:10.1038/nsb906.

Structural insights into the U-box, a domain associated with multi-ubiquitination

Melanie D. Ohi[1,2,3], **Craig W. Vander Kooi**[3,4,5], **Joshua A. Rosenberg**[1,2], **Walter J. Chazin**[4,5,6], and **Kathleen L. Gould**[1,2]

[1]Howard Hughes Medical Institute, Vanderbilt University, Nashville, Tennessee 37232, USA

[2]Department of Cell Biology, School of Medicine, Vanderbilt University, Nashville, Tennessee 37232, USA

[4]Department of Biochemistry, Vanderbilt University, Nashville, Tennessee 37232, USA

[5]Center for Structural Biology, Vanderbilt University, Nashville, Tennessee 37232, USA

[6]Department of Physics, Schools of Medicine and Arts & Science, Vanderbilt University, Nashville, Tennessee 37232, USA

Abstract

The structure of the U-box in the essential *Saccharomyces cerevisiae* pre-mRNA splicing factor Prp19p has been determined by NMR. The conserved zinc-binding sites supporting the cross-brace arrangement in RING-finger domains are replaced by hydrogen-bonding networks in the U-box. These hydrogen-bonding networks are necessary for the structural stabilization and activity of the U-box. A conservative Val→Ile point mutation in the Prp19p U-box domain leads to pre-mRNA splicing defects *in vivo*. NMR analysis of this mutant shows that the substitution disrupts structural integrity of the U-box domain. Furthermore, comparison of the Prp19p U-box domain with known RING–E2 complex structures demonstrates that both U-box and RING-fingers contain a conserved interaction surface. Mutagenesis of residues at this interface, while not perturbing the structure of the U-box, abrogates Prp19p function *in vivo*. These comparative structural and functional analyses imply that the U-box and its associated ubiquitin ligase activity are critical for Prp19p function *in vivo*.

Ubiquitin (Ub) targeting of proteins for degradation by the proteosome involves poly-ubiquination of substrate proteins *via* an enzyme cascade consisting of activating (E1), conjugating (E2) and ligating (E3) enzymes. E3 ubiquitin ligases vary widely in size, composition and enzymology, reflecting their regulatory role in substrate recognition[1]. HECT and RING finger domain–containing proteins constitute two classes of E3 ligases. HECT domains bind Ub through a thioester bond and transfer Ub directly to substrate. RING finger E3s facilitate the transfer of Ub from the E2 to the substrate, rather than binding Ub directly.

Correspondence should be addressed to K.L.G. kathy.gould@mcmail.vanderbilt.edu or W.J.C. walter.chazin@vanderbilt.edu.

[3]These authors contributed equally to this work.

Competing interests statement The authors declare that they have no competing financial interests.

A third class of E3 ubiquitin ligases has been recently identified[2,3]. This class of proteins contains a U-box motif, first identified in *Saccharomyces cerevisiae* Ufd2p. Ufd2p promotes the elongation of poly-ubiquitin chains in a U-box–dependent manner (recently termed an 'E4' activity)[4]. An alignment of U-boxes and RING motifs indicated that U-boxes lack the strictly conserved histidine and cysteine Zn^{2+}-chelating residues found in RING fingers, but they share a similar pattern of hydrophobic and polar amino acids (Fig. 1*a*), raising the possibility that they have similar folds[5].

S. cerevisiae Prp19p is an essential pre-mRNA splicing factor that contains an N-terminal U-box[6,7]. Interestingly, a mutation within the Prp19p U-box that results in the substitution of an isoleucine for a conserved valine (*prp19-1*) leads to pre-mRNA splicing defects and the disruption of several key protein–protein interactions within the spliceosome[8,9]. The profound physiological consequences that result from this mutation underscore the importance of the U-box motif for Prp19p function and premRNA splicing. Here we present the solution structure of the Prp19p U-box. In addition, the structural and functional consequences of mutations to different structural components of the Prp19 U-box were examined.

Comparison of U-box and RING fingers

A Prp19p fragment containing the U-box (residues 1–73) was produced for structure determination by NMR spectroscopy. NMR resonances were assigned using conventional heteronuclear strategies with ^{13}C,^{15}N-enriched protein[10]. Only the N-terminal 54 residues of Prp19p(1–73) form a well-folded structural domain. The threedimensional structure of residues 1–56 of the Prp19p U-box (Fig. 1*b*) was determined from a total of 859 NOE-derived distance constraints, 14 hydrogen bond constraints and 53 backbone dihedral angle constraints. A family of 50 starting structures calculated by a torsion angle dynamics algorithm was refined by restrained molecular dynamics, and the 20 structures with lowest violation energy were selected (Fig. 1*c*). The U-box domain is well defined, with an r.m.s. deviation *versus* the mean of 0.27 Å for the backbone atoms and 0.83 Å for all heavy atoms and 98% of all residues in the allowed regions of the Ramachandran plot.

The Prp19p U-box contains a central α-helix (residues Leu28–Gly36), a single turn of helix (Ser46–Glu49), four β-strands and a hydrophobic core involving Phe23, Leu28, Ile40, Ile47 and Ile50 (Fig. 1*b*). Three of the β-strands form a mini-antiparallel β-sheet composed of Arg12–Leu15, Thr21–Glu24 and Ile50–Ile53. The fourth β-strand (Asn37–Ile40) is packed against a nonregular loop. This organization is similar to the RING-fold that consists of a central α-helix and a series of loops of variable length interspersed with small β-strands[11–16]. Although residues 55–70 lack defined structure as determined by the number and range of observable NOEs, they show a substantial degree of line broadening, which reduces the crosspeak signal-to-noise (S/N) ratio in the NMR spectra. In contrast, residues 71–73 have sharp lines characteristic of a flexible unrestrained peptide-like character in solution. These observations suggest that amino acids 55–70 likely exchange among a number of conformations. The Prp19p-binding sites for pre-mRNA splicing factors Snt309p in *S. cerevisiae* and Cwf7p in *Schizosaccharomyces pombe* have been mapped to residues 63–73 (ref. 9). The conformational exchange in this region of Prp19p is likely to be

quenched upon binding, which would imply a functional role in finetuning interactions with target proteins.

Because hPrp19p has been shown to have E3 ligase activity[17], we compared the Prp19p U-box structure with that of three E3-type RING fingers: c-Cbl[14], RBX1 (ref. 15) and BRCA1 (ref. 16). The remarkable similarity between the Prp19p U-box and RING domains is illustrated using c-Cbl as a representative RING (Fig. 1*d,e*).

Stabilization by hydrogen-bond networks

The chelation of Zn^{2+} ions is fundamental to the stabilization of RING domains. Although the U-box lacks the ability to bind Zn^{2+}, analysis of the three-dimensional structure of the Prp19p U-box reveals that its fold is stabilized by networks of hydrogen bonds and salt bridges (Fig. 2*a*) in the same locations as the Zn^{2+}- binding sites in RING domains (Fig. 2*b*). Direct experimental evidence supporting this conclusion was obtained from the slowed solvent-exchange kinetics of protons involved in these networks. In particular, extraordinarily slow exchange was observed for the sulfhydryl and hydroxyl groups of Cys3 and Thr41. The ^{1}H NMR resonances of these two groups are observed as sharp lines at 6.01 and 5.82 p.p.m, which is rare in proteins and constitutes strong evidence of participation in hydrogen bonds. These observations, combined with the numerous NOE connectivities to the residues involved and the resultant hydrogen bonds in the structure, provide direct experimental confirmation of the hydrogen-bonding networks.

In one network, the Cys3 side chain is positioned between the backbone carbonyl of Lys8 and side chain carboxylate of Glu24, and other residues involved include Ser6, Arg11 and Ser26 (Fig. 2*c*). Cys3, Ser6, Glu24 and Ser26 correspond to four Zn^{2+}-chelating residues in RING domain proteins (Fig. 2*e*). In the other hydrogen-bonding network, the Thr41 side chain is positioned near the side chain carboxylate of Asp38, and other residues involved include Ser16, Ser19 and Ser46 (Fig. 2*d*). Residues Ser19, Asp38 and Thr41 correspond to three of the four Zn^{2+}- chelating residues in the corresponding site in RING domains (Fig. 2*e*). The fourth Zn^{2+} ligand in RING domains corresponds to Prp19p Thr21, which is at most only peripherally involved in the hydrogen-bonding network. Instead, other residues such as Ser16 and Ser46 are involved. Interestingly, the carboxylate side chain of Asp38 is at the center of this site and interacts with almost all of the other side chains, which is reminiscent of the role of the Zn^{2+} ion in the RING domain. The other site in the Prp19 U-box does not have such a well-defined focal point. An additional important feature of the hydrogen-bonding/salt-bridge networks is that these interactions should be dynamic in solution. This is reflected in part by the observation that not all conformers in the structural ensemble have identical hydrogen bond donor-acceptor pairs. Nevertheless, all conformers do have both hydrogen-bonding networks. In summary, we find the U-box is stabilized by a more decentralized (and likely dynamic) set of hydrogen-bonding and salt-bridge interactions than that provided by the Zn^{2+} sites in RING domains.

To test the importance of the hydrogen-bonding networks in U-box stability, four key residues were mutated separately to alanine, and the ^{15}N-^{1}H HSQC NMR spectrum of the mutant U-boxes was determined and compared with wild type. Cys3 and Thr41 were

selected because it was clear from the slow solvent-exchange kinetics that their side chain functional groups were involved in hydrogen bonding. The other two residues mutated, Glu24 and Asp38, were selected because they interact strongly with Cys3 and Thr41. Asp38 was also mutated because it seemed to play a strategic role at the center of the stabilization network. ^{15}N-^{1}H HSQC NMR was used to assay the structure of the mutants because wild type Prp19p(1–73) contains well-dispersed resonances resulting from the variable chemical environment of the amides in a well-folded protein. In contrast, the collapse of resonance dispersion in the spectra for the C3A, E24A, D38A and T41A mutant proteins reveals that disruption of a single hydrogen bond in either network results in significant destabilization of the U-box structure (Fig. 2*f*).

Residues at the putative E2 interface

The crystal structures of c-Cbl and RBX1 RING domains show that each RING contains a shallow hydrophobic groove formed by residues in the α-helix and two loops[13,14]. In c-Cbl, this groove interacts with the E2 enzyme UbcH7 (ref. 13). When the Prp19p U-box domain is structurally aligned with these RING domains, a similar hydrophobic surface is seen that involves Ile5, Tyr31, Pro39 and Ile40 (Fig. 3*a,b*). Mutations in the U-box–containing proteins CHIP, KIAA0860 protein and Ufd2p that correspond to the Y31A and P39A mutations of Prp19p abolish *in vitro* E3 activity[17]. In addition to these hydrophobic residues, the position corresponding to Prp19p Asp34 in c-Cbl and the U-box protein, UIP5, has been identified as essential for E2 interactions[13,18,19].

To address the structural ramifications of mutations in the putative E2-binding region, we constructed Y31A, D34A and P39A mutants of the Prp19p U-box. The ^{15}N-^{1}H HSQC NMR spectrum of the mutant U-boxes was measured and compared with wild type (Fig. 3*c–f*). In the cases of Y31A and D34A, the U-box structure is not greatly perturbed (Fig. 3*d,e*), implying that these mutations will be useful to directly assess the Prp19p interaction with its presumed E2 ligand. In contrast, Prp19p P39A does not have a defined tertiary structure (Fig. 3*f*). U-box mutants corresponding to residues Asp34 and Pro39 have been used to study U-box–E2 interactions[17,19]. In the case of the proline mutant, our studies show that mutations at this position in the U-box most likely disrupt its structure rather than interfere specifically with E2 interactions.

Prp19p requires the U-box for function

The *prp19-1* point mutation encoding a V14I substitution[20] was identified in a genetic screen for splicing mutants[21]. Val14 is a part of the well-packed hydrophobic core of the U-box (Fig. 4*a*). Thus, we suspected that this mutation might cause a structural defect in the protein. Consequently, NMR analysis was carried out on the mutant protein. As with the mutants involving the hydrogen-bonding network, the ^{15}N-^{1}H HSQC spectrum of Prp19-1p (1–73) (Fig. 4*b*) shows limited dispersion and decreased linewidth compared with the wild type protein, indicating loss of well-defined tertiary structure. Detailed analysis of the U-box structure revealed Val14 is so well packed that extension of the side chain by one methylene group at this position, converting Val to Ile, is sufficient for destabilizing the central hydrophobic core. Indeed, the F23G mutation of the central core residue also disrupts U-box

structure (data not shown) and Prp19p function (Table 1). These results show that the defects found in *prp19-1* are caused by U-box destabilization.

Six mammalian U-box–containing proteins, including hPrp19p, have been tested and found to show E3 ubiquitin ligase activity *in vitro*[17,22,23]. Similar to hPrp19p, *S. cerevisiae* Prp19p promoted the ligation of ubiquitin to proteins in an ubiquitin ligase reaction (Fig. 4*c*), whereas no ubiquitination products were observed in the presence of a mock reaction or in the absence of recombinant E1 and E2 enzymes (Fig. 4*c*). To determine whether the U-box is essential for this activity, we tested Prp19-1p, which contains the V14I substitution, and a U-box deletion mutant, Prp19p(64–504). These mutations abolished activity (Fig. 4*d,e*).

To determine whether the E3 ligase activity of Prp19p corresponds to its function *in vivo*, U-box mutations and truncations were introduced into the full-length *PRP19* gene. These *prp19* mutants, along with wild type *PRP19,* were then assayed for their ability to complement the null allele of *prp19* (*PRP19* is an essential gene) by a conventional plasmid shuffle approach. As expected, deletion of the entire U-box of Prp19p disrupted protein function *in vivo* (Table 1). Also, mutations in the hydrogen-bonding networks that destabilize the protein structure caused loss of function (Table 1). Interestingly, the D34A and Y31A mutants, which are predicted to interrupt the interaction with an E2, were also unable to rescue *prp19Δ* (Table 1). Because these mutations do not alter U-box structure (Fig. 3*d,e*) but do alter the interaction surface conserved between RING-finger and U-box proteins, these single amino acid substitutions likely eliminate the ability of the U-box to interact with its ligand, presumably an E2 enzyme.

The U-box and ubiquitination

U-box proteins are far less abundant than RING finger proteins in most eukaryotes, with only two encoded by the *S. cerevisiae* genome. The U-box proteins CHIP and *S. cerevisiae* Ufd2p clearly function *in vivo* by stimulating multi-ubiquitination in conjunction with specific E2 proteins[4,22,24,25]. Interestingly, it was recently reported that CHIP, like Ufd2p, is able to perform as an E4 ligase in addition to displaying *in vitro* E3 ligase activity[25]. This suggests that E4 activity may be a common feature of U-box proteins. If so, the structural analysis of the U-box provided here will allow the basis of E4 activity to be examined in more detail.

Ubiquitination plays various roles in the cell. Although many poly-ubiquitinated proteins are rapidly degraded by the 26S proteosome, ubiquitination can create a regulatory, rather than a proteolytic, signal[1]. Prp19p is essential for pre-mRNA splicing and is present in a complex that contains many proteins[9,26]. Thus far, however, its biochemical role in pre-mRNA splicing and that of the proteins with which it interacts are unknown. The combined functional and structural analyses presented here strongly suggest that Prp19p acts as an ubiquitin ligase *in vivo*, setting the foundation to explore the role of ubiquitination in pre-mRNA splicing.

Methods

Expression and purification of Prp19p(1–73) fragments for NMR analysis

Recombinant Prp19p(1–73) fused to a N-terminal His_6-tag and its indicated mutants were generated by PCR sitedirected mutagenesis and expressed in *Escherichia coli* BL21 (pLysS) (Novagen). All mutants were confirmed by DNA sequencing. Samples enriched in ^{13}C and ^{15}N were produced by growth in M9 minimal media with ^{13}C-glucose and $^{15}NH_4Cl$ as the sole carbon and nitrogen sources. Cells were lysed in 20 mM Tris-HCl, pH 8.0, 100 mM NaCl, 1 mM EDTA and 5 mM dithiothreitol (DTT), and proteins were purified using Ni^{2+}-nitrilotriacetic acid (Ni^{2+}-NTA) columns (Qiagen) following the manufacturer's instructions. The His_6-tag was cleaved by incubation with thrombin (25 U per −20 mg protein) for 4 h at room temperature. The Prp19p(1–73) proteins were further purified using a Mono-Q 10/10 column (20 mM sodium phosphate, pH 7.0, elution 10–300 mM NaCl) (Amersham Pharmacia Biotech). NMR spectra were recorded on 1 mM protein samples in 20 mM sodium phosphate, pH 7.0, 20 mM NaCl and 5 mM DTT.

NMR spectroscopy and resonance assignments

NMR experiments were performed on Bruker Avance spectrometers operating at 600 and 800 MHz proton frequencies. Experiments were carried out at 30 °C for Prp19p(1–73) and 25 °C for the mutants. Sequencespecific backbone assignments were made using ^{15}N,^{13}C-labeled Prp19p(1–73) using standard triple-resonance experiments[10]. Side chain assignments were obtained from 2D ^{1}H COSY and TOCSY as well as 3D HCCH-TOCSY spectra.

Proton-proton distance constraints were derived from three NOESY spectra: a 2D homonuclear ^{1}H NOESY spectrum (τ_m = 100 ms), a 3D ^{15}N-resolved [^{1}H, ^{1}H] NOESY (τ_m = 100 ms) and a 3D ^{13}C-resolved [^{1}H, ^{1}H] NOESY (τ_m = 100 ms). Data was processed using XWINNMR (Bruker) and analyzed using XEASY[27]. The solution structure of Prp19p(1–73) was determined using NOE-derived distance constraints and torsion angle constraints derived from chemical shifts using TALOS[28]. Torsion angle dynamics calculations were performed using DYANA[29], followed by restrained molecular dynamics using AMBER[30] following established protocols[31–33]. A summary of structural statistics is provided in Table 2.

Ubiquitination assays

The *in vitro* ubiquitination assay was performed as described[17] with some modifications. In brief, empty pSK(+), pSK(+)PRP19 (pKG1781), pSK(+)*prp19-1* (pKG177) or pSK(+)PRP19(64–504) (pKG550) were translated *in vitro* in the presence of [^{35}S]-Trans label (ICN Pharmaceuticals) with the use of the T_NT-Coupled Reticulocyte Lysate System (Promega). *In vitro* translated, ^{35}S-labeled Prp19p, ^{35}S-labeled Prp19p-1, ^{35}S-labeled Prp19p (64–504) or mock reaction (3 μl each) was combined with 0.1 μg His_6-E1, 1 μg His_6-Ubc3, 0.5 units phosphocreatine kinase, 1 μg ubiquitin (Sigma), 25 mM Tris-HCl, pH 7.5, 120 mM NaCl, 2 mM ATP, 1 mM $MgCl_2$, 0.3 mM DTT and 1 mM creatine phosphate (20 μl total reaction volume). Reactions were incubated for 2 h at room temperature and terminated by the addition of SDS sample buffer. One portion of the sample was resolved on 10% SDS-PAGE gels, transferred to a PVDF membrane, and subjected to immunoblot

analysis with a rabbit polyclonal antibody to ubiquitin (Sigma) at a 1:100 dilution. After western anaylsis, blots were exposed to PhosphorImager screens and visualized using ImageQuant (version 3.3) (Molecular Dynamics). Another portion was resolved on 10% SDS-PAGE gels, and the proteins were visualized by fluorography.

Strains and media

A *prp19:HIS3 ura3-52 leu2-Δ* haploid strain carrying a *URA3*-selectable vector expressing wild type *PRP19* was transformed by a standard lithium acetate method with *PRP19* cDNA and mutants under control of the *GAL1* promoter in a *LEU2*-based vector. Ura^+ Leu^+ transformants were streaked to plates containing 5-fluorourotic acid to score the ability of *prp19* mutations to rescue growth of the *prp19Δ* strain.

Coordinates

Coordinates for the ensemble of structures have been deposited at the Protein Databank (accession code 1N87). The NMR chemical shifts have been deposited in the BMRB (accession code 5594).

Acknowledgments

We thank S. Hatakeyama and K.I. Nakayama from the Department of Molecular and Cellular Biology at Kyushu University for the kind gift of GST-Ubc3. We also gratefully acknowledge J.A. Smith for valuable technical assistance with structure calculations and molecular graphics. Work in our laboratories was supported by the National Institutes of Health in the form of operating grants to K.L.G. and W.J.C., training grant positions to M.D.O., C.W.V.K. and J.A.R., and core facility grants to the Vanderbilt Ingram Cancer Center and the Vanderbilt Center in Molecular Toxicology. K.L.G. is an Associate Investigator of the Howard Hughes Medical Institute.

References

1. Pickart CM. Mechanisms underlying ubiquitination. Annu. Rev. Biochem. 2001; 70:503–533. [PubMed: 11395416]
2. Cyr DM, Hohfeld J, Patterson C. Protein quality control: U-box-containing E3 ubiquitin ligases join the fold. Trends Biochem. Sci. 2002; 27:368–375. [PubMed: 12114026]
3. Patterson, C. A new gun in town: the U box is a ubiquitin ligase domain. Sci. STKE. 2002. [online]<http://stke.sciencemag.org/cgi/content/full/OC_sigtraus;2002/116/pe4>
4. Koegl M, et al. A novel ubiquitination factor, E4, is involved in multiubiquitin chain assembly. Cell. 1999; 96:635–644. [PubMed: 10089879]
5. Aravind L, Koonin EV. The U box is a modified RING finger — a common domain in ubiquitination. Curr. Biol. 2000; 10:R132–R134. [PubMed: 10704423]
6. Tarn WY, Lee KR, Cheng SC. Yeast precursor mRNA processing protein PRP19 associates with the spliceosome concomitant with or just after dissociation of U4 small nuclear RNA. Proc. Natl. Acad. Sci. USA. 1993; 90:10821–10825. [PubMed: 8248176]
7. McDonald WH, Ohi R, Smelkova N, Frendewey D, Gould KL. Myb-related fission yeast Cdc5p is a component of a 40S snRNP-containing complex and is essential for pre-mRNA splicing. Mol. Cell. Biol. 1999; 19:5352–5362. [PubMed: 10409726]
8. Chen HR, et al. Snt309p, a component of the Prp19p-associated complex that interacts with Prp19p and associates with the spliceosome simultaneously with or immediately after dissociation of U4 in the same manner as Prp19p. Mol. Cell. Biol. 1998; 18:2196–2204. [PubMed: 9528791]
9. Ohi MD, Gould KL. Characterization of interactions among the Cef1p-Prp19p-associated splicing complex. RNA. 2002; 8:798–815. [PubMed: 12088152]
10. Cavanagh, J., Fairbrother, WJ., Palmer, AG., Skelton, NJ. Protein NMR Spectroscopy: Principles and Practice. Academic Press; San Diego: 1996.

11. Gervais V, et al. Solution structure of the N-terminal domain of the human TFIIH MAT1 subunit: new insights into the RING finger family. J. Biol. Chem. 2001; 276:7457–7464. [PubMed: 11056162]
12. Hanzawa H, et al. The structure of the C4C4 ring finger of human NOT4 reveals features distinct from those of C3HC4 RING fingers. J. Biol. Chem. 2001; 276:10185–10190. [PubMed: 11087754]
13. Bellon SF, Rodgers KK, Schatz DG, Coleman JE, Steitz TA. Crystal structure of the RAG1 dimerization domain reveals multiple zinc-binding motifs including a novel zinc binuclear cluster. Nat. Struct. Biol. 1997; 4:586–591. [PubMed: 9228952]
14. Zheng N, Wang P, Jeffrey PD, Pavletich NP. Structure of a c-Cbl-UbcH7 complex: RING domain function in ubiquitin-protein ligases. Cell. 2000; 102:533–539. [PubMed: 10966114]
15. Zheng N, et al. Structure of the Cul1–Rbx1–Skp1–F boxSkp2 SCF ubiquitin ligase complex. Nature. 2002; 416:703–709. [PubMed: 11961546]
16. Brzovic PS, Rajagopal P, Hoyt DW, King MC, Klevit RE. Structure of a BRCA1–BARD1 heterodimeric RING–RING complex. Nat. Struct. Biol. 2001; 8:833–837. [PubMed: 11573085]
17. Hatakeyama S, Yada M, Matsumoto M, Ishida N, Nakayama KI. U box proteins as a new family of ubiquitin-protein ligases. J. Biol. Chem. 2001; 276:33111–33120. [PubMed: 11435423]
18. Huang L, et al. Structure of an E6AP-UbcH7 complex: insights into ubiquitination by the E2–E3 enzyme cascade. Science. 1999; 286:1321–1326. [PubMed: 10558980]
19. Pringa E, Martinez-Noel G, Muller U, Harbers K. Interaction of the ring finger-related U-box motif of a nuclear dot protein with ubiquitin-conjugating enzymes. J. Biol. Chem. 2001; 276:19617–19623. [PubMed: 11274149]
20. Chen HR, et al. Snt309p, a component of the Prp19p-associated complex that interacts with Prp19p and associates with the spliceosome simultaneously with or immediately after dissociation of U4 in the same manner as Prp19p. Mol. Cell. Biol. 1998; 18:2196–2204. [PubMed: 9528791]
21. Vijayraghavan U, Company M, Abelson J. Isolation and characterization of pre-mRNA splicing mutants of *Saccharomyces cerevisiae*. Genes Dev. 1989; 3:1206–1216. [PubMed: 2676722]
22. Jiang J, et al. CHIP is a U-box-dependent E3 ubiquitin ligase: identification of Hsc70 as a target for ubiquitylation. J. Biol. Chem. 2001; 276:42938–42944. [PubMed: 11557750]
23. Murata S, Minami Y, Minami M, Chiba T, Tanaka K. CHIP is a chaperone-dependent E3 ligase that ubiquitylates unfolded protein. EMBO Rep. 2001; 2:1133–1138. [PubMed: 11743028]
24. Meacham GC, Patterson C, Zhang W, Younger JM, Cyr DM. The Hsc70 co-chaperone CHIP targets immature CFTR for proteasomal degradation. Nat. Cell. Biol. 2001; 3:100–105. [PubMed: 11146634]
25. Imai Y, et al. CHIP is associated with Parkin, a gene responsible for familial Parkinson's disease, and enhances its ubiquitin ligase activity. Mol. Cell. 2002; 10:55–67. [PubMed: 12150907]
26. Tarn WY, et al. Functional association of essential splicing factor(s) with PRP19 in a protein complex. EMBO J. 1994; 13:2421–2431. [PubMed: 8194532]
27. Bartels C, Xia T, Billeter M, Guntert P, Wuthrich K. XEASY. J. Biomol. NMR. 1995; 6:1–10. [PubMed: 22911575]
28. Cornilescu G, Delaglio F, Bax A. Protein backbone angle restraints from searching a database for chemical shift and sequence homology. J. Biomol. NMR. 1999; 13:289–302. [PubMed: 10212987]
29. Guntert P, Mumenthaler C, Wuthrich K. Torsion angle dynamics for NMR structure calculation with the new program DYANA. J. Mol. Biol. 1997; 273:283–298. [PubMed: 9367762]
30. Pearlman, DA., et al. AMBER 4.1. San Francisco, CA: University of California, San Francisco; 1995.
31. Maler L, Potts BC, Chazin WJ. High resolution solution structure of apo calcyclin and structural variations in the S100 family of calcium-binding proteins. J. Biomol. NMR. 1999; 13:233–247. [PubMed: 10212984]
32. Maler L, Blankenship J, Rance M, Chazin WJ. Site-site communication in the EF-hand Ca^{2+}-binding protein calbindin D9k. Nat. Struct. Biol. 2000; 7:245–250. [PubMed: 10700285]
33. Sastry M, et al. The three-dimensional structure of Ca^{2+}-bound calcyclin: implications for Ca^{2+}-signal transduction by S100 proteins. Structure. 1998; 6:223–231. [PubMed: 9519412]

34. Lackner P, Koppensteiner WA, Sippl MJ, Domingues FS. ProSup: a refined tool for protein structure alignment. Protein Eng. 2000; 13:745–752. [PubMed: 11161105]

35. Koradi R, Billeter M, Wuthrich K. MOLMOL: a program for display and analysis of macromolecular structures. J. Mol. Graph. 1996; 14:51–55. [PubMed: 8744573]

36. Laskowski RA, Rullman JA, MacArthur MW, Kaptein R, Thornton JM. AQUA and PROCHECK-NMR: programs for checking the quality of protein structures solved by NMR. J. Biomol. NMR. 1996; 8:477–486. [PubMed: 9008363]

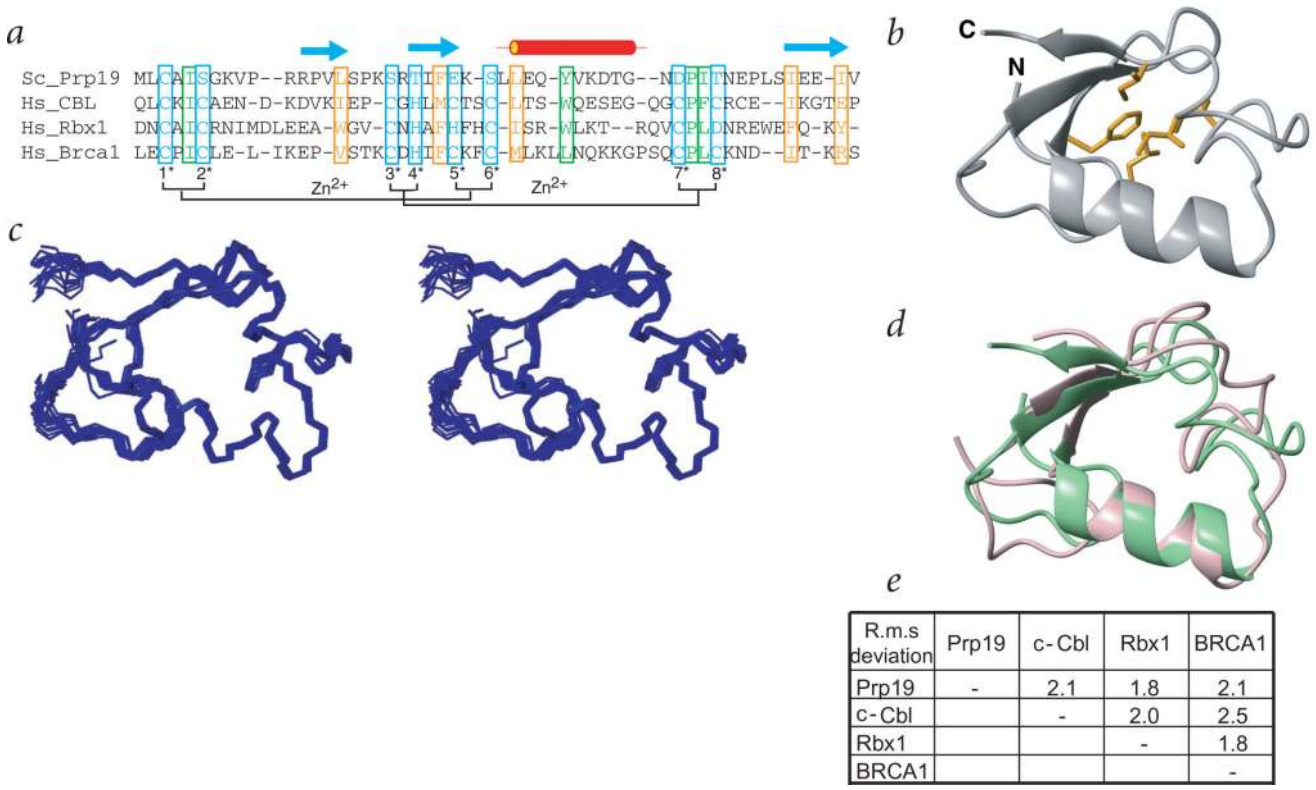

R.m.s deviation	Prp19	c-Cbl	Rbx1	BRCA1
Prp19	-	2.1	1.8	2.1
c-Cbl		-	2.0	2.5
Rbx1			-	1.8
BRCA1				-

Fig. 1.

The U-box and RING finger domains share a conserved fold. ***a***, Alignment of selected U-box and RING finger domains. The shadings are yellow for hydrophobic, green for residues important in c-Cbl interaction with its E2 and blue for Zn^{2+}-chelating residues in the RING fingers. Hs represents human proteins; Sc, *S. cerevisiae*. Blue arrows above the alignment indicate β-strands, and the red cylinder indicates the central α-helix. ***b***, Ribbon diagram of the three-dimensional structure of the Prp19p U-box domain, with core hydrophobic residues in yellow. ***c***, Stereo view of the Cα trace of the 20 lowest energy NMR structures. ***d***, Overlay of the structures of the Prp19p U-box (green) and the c-Cbl RING finger (pink) (PDB entry 1FBV). ***e***, Backbone r.m.s. deviations between the Prp19p U-box and three RING fingers using ProSup[34]. Panels (*b*–*d*) were generated using MolMol[35].

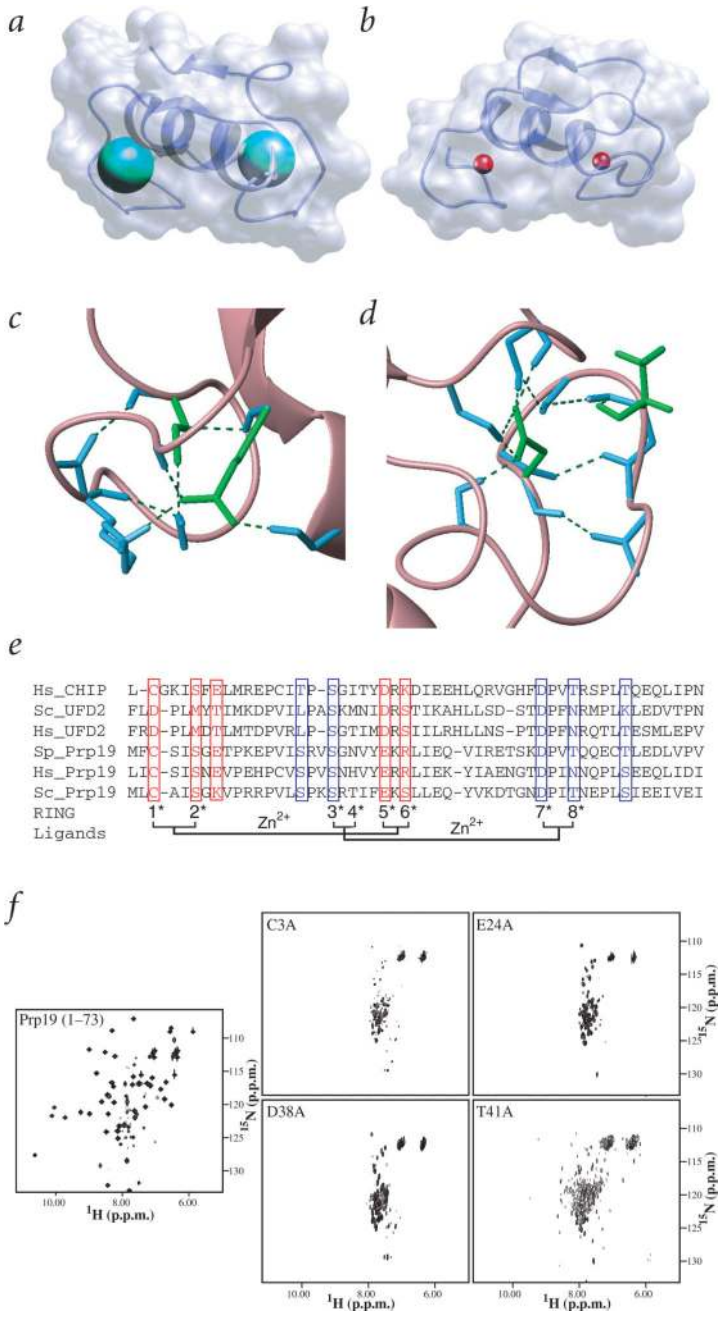

Fig. 2.

U-box stability is mediated by hydrogen-bonding networks. ***a***, Structure of the Prp19p U-box with the hydrogen-bonding networks represented by a green sphere with a radius of 2.7 Å. Sphere centers are located at the sulfhydryl of Cys3 and carboxylate of Asp38. ***b***, Structure of the c-CBL RING finger with zinc ions represented by a red sphere with a van der Waals radius of 1.3 Å. ***c***,***d***, Residues involved in the first and second hydrogen-bonding networks. Shown is an optimized close-up view of the two networks in the Prp19p U-box, with donor-acceptor distances ≤2.7 Å highlighted by green dotted lines. Residues selected for subsequent mutagenesis are displayed in green. ***e***, Sequence alignment of several U-box

proteins. The eight positions of the zinc ligands in RING proteins are indicated below. Residues structurally identified as participating in the two hydrogen-bonding networks are shown in red and blue. ***f***, ^{15}N-^{1}H HSQC spectra of Prp19p(1–73) and the C3A, E24A, D38A and T41A mutants.

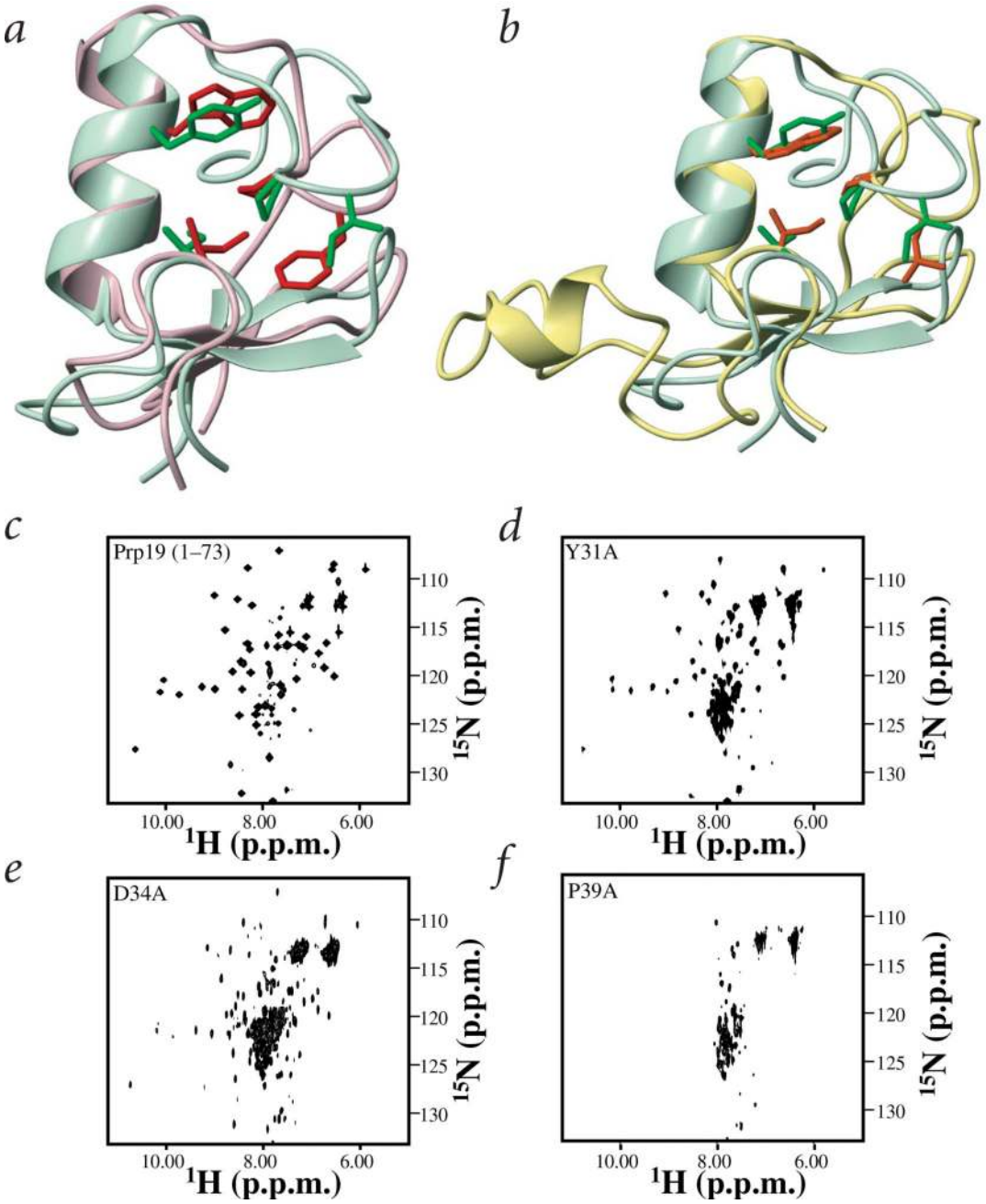

Fig. 3.

Mutational analysis of putative E2-interacting residues in the U-box. ***a***, Overlay of the three-dimensional structures of the Prp19p U-box (green) and the c-Cbl RING finger (pink) (PDB entry 1FBV). Residues found in the shallow hydrophobic groove are indicated in green for the U-box and in red for c-Cbl. ***b***, Overlay of the three-dimensional structures of the Prp19p U-box (green) and the Rbx1 E3-type RING finger (yellow) (PDB entry 1LDJ). Residues found in the shallow hydrophobic groove are shown in green for the U-box and in red for Rbx1. ^{15}N-^{1}H HSQC spectra of ***c***, Prp19p(1–73) and the ***d***, Y31A; ***e***, D34A; and ***f***, P39A mutants.

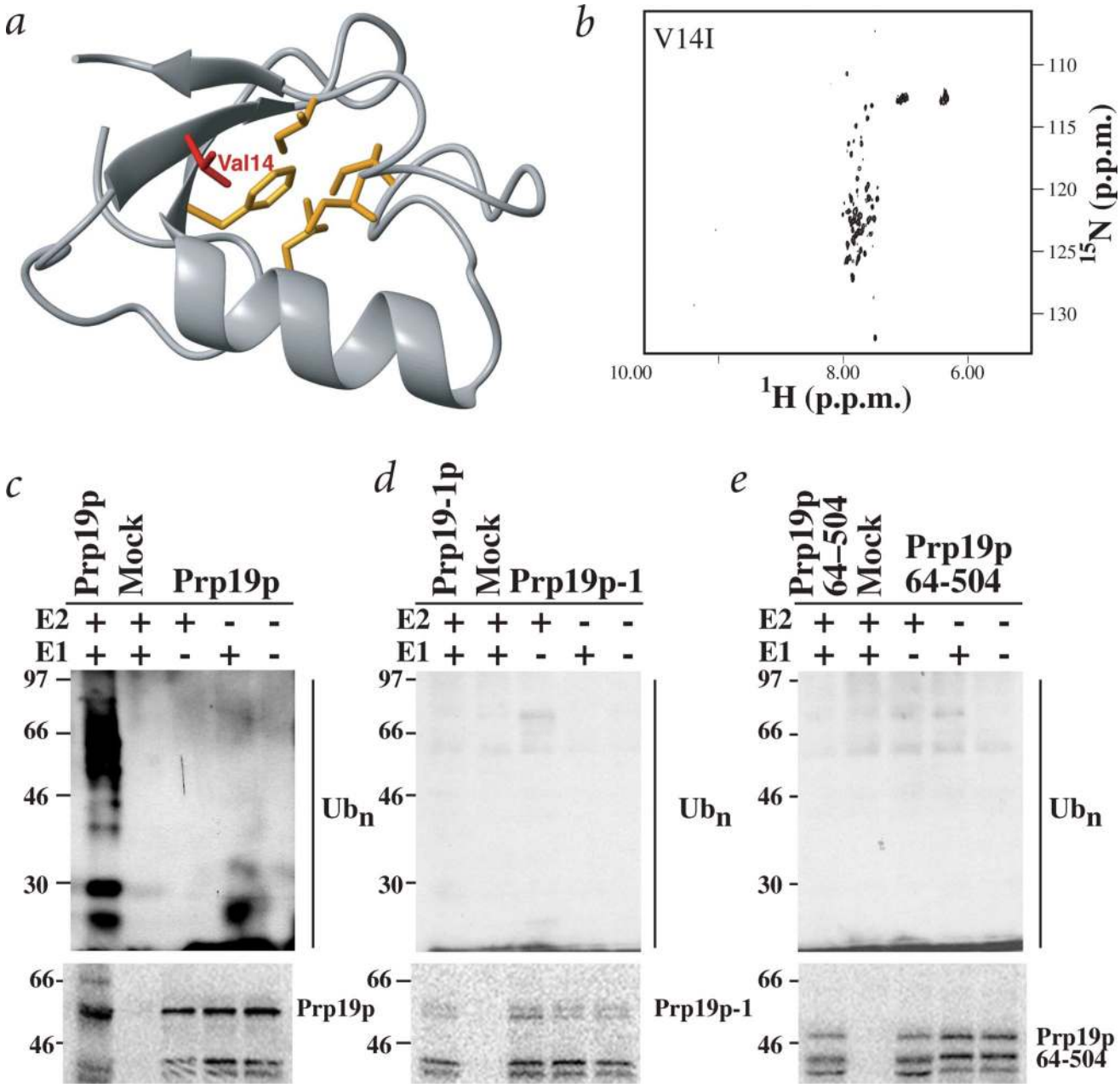

Fig. 4.

The U-box domain is required for Prp19p function. ***a***, Ribbon diagram of the U-box structure. The Val14 side chain is red, and the side chains of Phe23, Leu28, Ile40, Ile47 and Ile50 are yellow. Val14 has a central role in the protein core, forming extensive contacts with Phe23 and Leu28 in the hydrophobic core, as well as with the aliphatic portions of Lys25 and Glu52, which are solvent exposed. ***b***, ^{15}N-^{1}H HSQC spectrum of Prp19-1p(1–73). Ubiquitination assays preformed with *in vitro* transcribed and translated ***c***, Prp19p; ***d***, Prp19-1p; or ***e***, Prp19p(64–504). Controls lacking recombinant E1, E2 (Ubc3) and/or Prp19 proteins are indicated in each panel with a minus sign. The reaction mixtures were resolved under reducing conditions by SDS-PAGE, and the separated proteins were subjected to

immunoblot analysis with antibodies to ubiquitin (upper panels) or visualized directly by autoradiography (lower panels).

Table 1

Consequence of mutations *in vivo*

	Consequence *in vitro*	Area of mutation	*prp19*Δ *in vivo* rescue
Prp19	Positive control	Wild type	+
VECTOR	Negative control	–	–
Prp19(64–504)	Negative control	U-box delete	–
F23G	Misfolded	Hydrophobic core	–
C3A	Misfolded	Hydrogen bond	–
E24A	Misfolded	Hydrogen bond	–
D38A	Misfolded	Hydrogen bond	–
T41A	Misfolded	Hydrogen bond	–
Y31A	Well folded	Putative E2 interface	–
D34A	Well folded	Putative E2 interface	–
P39A	Misfolded	Putative E2 interface	–

Table 2

Structural statistics[1] of the Prp19p U-box

Restraints for calculation	
Total NOE restraints	859
Intraresidue	225
Sequential	213
Medium Range	160
Long range	261
Hydrogen bonds	14
Dihedral angle constraints	53
Constraint violations (mean and s.d.)	
Distance constraints ≤0.2 Å	0.4 ± 0.5
Dihedral angle constraint violations ≤5°	0.9 ± 0.7
Maximum distance constraint violation	0.19 ± 0.03
Maximum dihedral constraint violation	6.3 ± 3.2
AMBER[2] energies (kcal mol^{-1})	
Constraint energy	17.8 ± 1.5
Total energy	−2,117 ± 12
Ramachandran statistics (%)[3]	
Most favored	77
Additionally allowed	20
Generously allowed	1
Disallowed	2
R.m.s. deviation from mean structure (Å)	
Backbone atoms	0.27
All heavy atoms	0.83

[1] Structure statistics refers to an ensemble of 20 structures with the lowest energy from 50 calculated structures.

[2] See ref. 30.

[3] Statistics for the mean coordinates after restrained molecular dynamics determined with PROCHECK-NMR[36].